

UWB Channel Modeling for BANs based on the ARMA Synthesis Method

Marco Hernandez, Takahiro Aoyagi, Juni-chi Takada, Ryuji Kohno
Medical Information and Communications Technology Group
National Institute of Communications and Information Technologies
3-4 Hikarino-oka, Yokosuka
239-0847 Japan
Marco@nict.go.jp

Abstract—As UWB channels for BANs behave as linear systems, an alternative form of channel modeling is by linear prediction of the channel's transfer function obtained from measurements. The main reason of this is a more accurate reproduction of the channel transfer function with less parameters than conventional statistical channel models. In contrast to conventional statistical channel models, where channel impulse responses are constructed from a statistical characterization of multipath amplitudes, phases and delays arriving in clusters, etc., the channel impulse response derived from an ARMA channel model is more accurate than a statistical channel model. Indeed, as this ARMA channel model is derived directly from measured channel transfer functions. So, it is expected that this channel impulse response is more accurate. Recall, a statistical channel model has some degree of error depending how precise the statistical characterization was performed. Moreover, the whole propagation phenomena (large scale and small scale fading) are embedded in a *simple* model.

Index Terms—UWB channel modeling, body area networks (BANs), auto-regressive moving-average (ARMA) synthesis method.

I. Introduction

The wireless channel determines the system performance limits of BANs in both theory and practice. Thus, understanding and modeling such channels become an important prerequisite for designing and evaluating physical and MAC layer proposals for BANs.

Measurements reported in the literature of UWB channels around the human body indicate that some modifications are necessary in order to model BAN scenarios accurately. Indeed, due to the short distance between sensors on a human body and the close proximity to the human body, the UWB-BAN channel model has different path loss, amplitude distribution, clustering, and inter-arrival time characteristics compared to other UWB scenarios.

Moreover, as BANs employ special antennas attach to the human body either wearable or on-body (patches), this proximity to the human body changes the antenna's characteristics. Consequently, the dynamic characteristics of propagation are difficult to study as those depend from person to person and how antennas are handle. Hence, the effects of body and antennas into the propagation channel are not separated or decouple as in conventional channel measurements. The dynamics of both antennas and human body are characterized into one entity and embedded into the propagation channel.

On the other hand, UWB channels for BANs are assumed as linear system as in any other wireless channel. Thus, an alternative form of channel modeling is by linear prediction of the channel's transfer function obtained from measurements. The main reason of this is a more accurate reproduction of the channel transfer function with less parameters than conventional statistical channel models.

Besides, the whole propagation phenomena (large scale and small scale fading) are embedded in a *simple* model. Moreover, reproducing channel impulse responses in a computer for simulations is fairly straight forward.

II. UWB Channel Measurements

A common method of radio channel's characterization is by exploiting its linear property. Assuming an output-input relationship given by

$$y(t) = \int x(t - \tau) h(t, \tau) d\tau \quad (1)$$

where $x(t)$ is the input signal, $y(t)$ is the output signal and $h(t, \tau)$ is the time variant channel's impulse response. In terms of the time variant transfer function $T(f, t)$, the output-input relationship is given by

$$y(t) = \int X(f) T(f, t) \exp(2\pi f t) df \quad (2)$$

A frequency domain characterization can be obtained by an input signal localized in the frequency domain, i.e., $X(f) = \delta(f - f_0)$ such that

$$y(t) = T(f_0, t) \exp(j2\pi f_0 t) \quad (3)$$

If the channel is slowly time varying

$$T(f, t) \approx T(f, t_0) \quad (4a)$$

for

$$|t - t_0| < 1/f_0 \quad (4b)$$

so that

$$y(t) \approx T(f_0, t_0) \exp(j2\pi f_0 t) \quad (5)$$

which leads to

$$Y(f) \approx T(f_0, t_0) \delta(f - f_0) = T(f_0, t_0) X(f) \quad (6)$$

Equation 6 is the output-input relationship in the frequency domain when the input has an impulse excitation. This quasi-static equation is measured by a vector network analyzer (VNA) through the scattering parameter S_{21} for a two port radio channel. Complexities of solving Maxwell equations to characterize the BAN channel are reduced to an output-input relation.

This technique has the advantage of calibrated measurements are performed relatively easy. Although, it has the serious disadvantage of a limited use for quasi-static channels only. Indeed, as the VNA employs IF filtering, f_0 in Equation 4b is replaced by the IF bandwidth, resulting in a stronger constrain for the VNA to capture the time variability of the channel under measurement.

A. Channel Measurements

The measurements for UWB channels were performed in the UWB band (3 GHz to 10 GHz) and UWB lower band (3 GHz to 5 GHz). The VNA recorded a snap shot of 3201 and 801 sampling points with a sampling frequency of 2 GHz. The employed antenna is skycross, which was placed in different positions in a human body. Measurements took place in an anechoic chamber and conventional hospital room.

III. Linear Prediction of Random Processes

The background of this approach is that the concentration or spread of the power spectrum indicates the correlated or random structure of a signal process. Thus, the power spectrum can be used to deduce the existence of correlated patterns or repetitive structures in the signal process. The literature is rich in spectrum analysis research works. In particular, linear model-based spectral estimation assumes a given signal $z(t)$ is modeled as the output of a linear system (radio channel) excited by a random, flat-spectrum excitation. Thus, the power spectrum of the model output is shaped entirely by the frequency response of the model. Hence, an input-output relation of a generalized discrete linear model is given by

$$z(m) = \sum_{k=1}^P a_k z(m-k) + \sum_{k=0}^Q b_k e(m-k) \quad (7)$$

where $z(m)$ is the model output, $e(m)$ is the input signal, $\{a_k\}$ and $\{b_k\}$ are the parameters of the model. Equation 7 is known as the autoregressive-moving average model (ARMA).

The frequency response of the model is given by

$$H(z) = \frac{B(z)}{A(z)} = \frac{\sum_{k=0}^Q b_k z^{-k}}{1 - \sum_{k=1}^P a_k z^{-k}} \quad (8)$$

with power spectrum

$$P_Z(f) = P_E(f) |H(f)|^2 \quad (9)$$

Assuming the input signal $e(m)$ is white noise with unit variance, the input power spectrum is $P_E = 1$ and so the power spectrum of the model output is the square magnitude of the frequency response of the model

$$P_Z = |H(f)|^2 \quad (10)$$

IV. Maximum Entropy Spectral Estimation

The power spectrum of a stationary signal is defined as

$$P_Z(f) = \sum_{m=-\infty}^{\infty} R_{xx}(m) \exp(-j2\pi fm) \quad (11)$$

that is, the Fourier transform of the autocorrelation sequence R_{xx} . Notice that such autocorrelation is defined for time-lags in the interval $(-\infty, +\infty)$, but in practice such interval is finite $(-P, P)$. In parametric methods, R_{xx} is assumed zero for $|m| > P$ for which no measure or estimate values are provided. This assumption results in spectral leakage and so loss in frequency resolution. Thus, nonparametric methods are introduced to overcome this disadvantage based on the maximum spectral estimation. Indeed, the maximum entropy estimate is based on the principle that the estimate of the autocorrelation sequence corresponds to the most random signal, whose correlation values in $|m| \leq P$ coincide with the measured values. In [1], it is shown that the maximum entropy power spectrum estimate is obtained by maximizing the entropy of the power spectrum with respect to the unknown autocorrelation values, such that

$$\hat{P}_Z^{\text{ME}} = \frac{\sigma^2}{A(z)A(z^{-1})} \quad (12)$$

That is, the maximum entropy power spectrum estimation is the power spectrum of an autoregressive model.

V. Autoregressive Power Spectrum Estimation

An autoregressive (AR) or linear prediction model is defined as

$$z(m) = \sum_{k=1}^P a_k z(m-k) + e(m) \quad (13)$$

where $e(m)$ is random with flat spectrum and variance σ_e^2 . The power spectrum of an autoregressive process is given by

$$P_Z^{\text{AR}}(f) = \frac{\sigma_e^2}{|1 - \sum_{k=1}^P a_k \exp(-j2\pi fk)|^2} \quad (14)$$

As mentioned before, the AR model extrapolates the correlation sequence beyond the range for which estimates are available. That is, the AR model is nonparametric. By multiplying both sides of Equation 13 by $z(m-j)$, taking expectation and noticing that $e(m)$ is orthogonal to past samples $z(m-j)$, we obtain

$$R_{zz}(j) = \sum_{k=1}^P a_k R_{zz}(j-k) ; j \in \mathbb{Z}^+ \quad (15)$$

Hence, given $P + 1$ correlation values, Equation 15 can be solved to obtain the AR coefficients $\{a_k\}$. Equation 15 can be used to extrapolate the correlation sequence as well. Indeed, by assuming the system model is casual (zero for $n < 0$), the autocorrelation R_{zz} can be expressed in terms of the AR model parameters as

$$R_{zz}(m) = \begin{cases} \sum_{k=1}^P a_k R_{zz}(m-k) & m \geq 0 \\ \sum_{k=1}^P a_k R_{zz}(m-k) + \sigma_e^2 & m = 0 \\ R_{zz}^*(-m) & m < 0 \end{cases} \quad (16)$$

Thus, if $P + 1$ correlation values are known ($R_{zz}(m)$ for $m = 0, 1, \dots, P$), the filter parameters can be found by solving P linear equations given by

$$\begin{bmatrix} R_{zz}(0) & \dots & R_{zz}(P) \\ R_{zz}(-1) & \dots & R_{zz}(P-1) \\ \vdots & & \vdots \\ R_{zz}(P) & \dots & R_{zz}(0) \end{bmatrix} \begin{bmatrix} 1 \\ a_1 \\ \vdots \\ a_P \end{bmatrix} = \begin{bmatrix} \sigma_e^2 \\ 0 \\ \vdots \\ 0 \end{bmatrix} \quad (17)$$

Equation 17 is known as the Yule-Walker equations.

Then, the AR model provides a practical method for signal process modeling. That is, if we want to represent a given random signal process $z(n)$ by the AR model, the correlation $R_{zz}(m)$ can be estimated and used in Equation 17 to solve for the model parameters $\{a_k\}$.

VI. AR Modeling of UWB-BAN Channels

Based on all above, the channel's transfer function $H(f_n)$ can be obtained in the frequency domain in terms of the measured scattering parameter S_{21} . We can characterize the random nature of the UWB channel by an AR process modeling as

$$H(f_n, d) = \sum_{i=1}^P a_i H(f_{n-i}, d) + e(f_n) \quad (18)$$

where $H(f_n, d)$ is the n th sample of the $|S_{21}|^2$ measurement in the frequency domain at location d . $e(f_n)$ is a white process with distribution $\mathcal{N}(0, \sigma_e^2)$.

Notice that the 1st and 2nd order statistics of the UWB channel are captured in the AR model. The advantage of this modeling respect to conventional time domain approaches is that less parameters are required to generate a simulation program that resembles the behavior of an UWB-BAN channel (including large and small scale fading), besides of being more accurate of a conventional statistical channel model. The main drawback is that it does not provide information about the phase.

A difference with similar approaches found in the literature, is that the statistical correlation R_{zz} is not estimated from the measured data (sample correlation) by rather estimated by the data-oriented least squares criterion, where the sum of square terms of a conditional likelihood function is minimized.

A. Large Scale Fading

As the UWB-BAN channel's transfer function can be simulated by Equation 18, it contains all the propagation phenomena

embedded. Thus, we can extract conventional channel model metrics as the path loss. The path loss is calculated by averaging the transfer functions over the frequency band as a function of the distance d as [5]:

$$PL(d) = -10 \text{Log}_{10} \frac{1}{NM} \sum_{m=1}^M \sum_{n=1}^N |H_m(f_n, d)|^2 \quad (19)$$

where M is the number of measured transfer functions at distance d and N is the number of sampling points in a snapshot.

For the sake of illustration, having measurements for certain positions, the path loss law can be computed as

$$PL(d) = P_0 + 10 n \text{Log} \left(\frac{d}{d_0} \right) + X \quad (20)$$

where P_0 is the path loss at reference distance d_0 and X is a random variable that introduces statistical variability. Notice that the path loss exponent n is obtained from a simple linear regression.

Once the path loss has been characterized for the link budget, it can be removed by normalizing the total energy of the channel impulse response to unity. Such that Equation 18 does not depend on d .

B. Small Scale Fading

The small scale fading is used to describe the rapid fluctuations of the radio signal over a short period of time, so that the large-scale path loss effects might be ignored. The small scale fading is related to the channel's impulse response that contains all the necessary information: 1) rapid changes in the signal strength, 2) random frequency modulation due to Doppler shifts and 3) time dispersion (echoes) caused by multipath propagation delays.

$$h(\tau) = \text{IFFT}\{H(f)\} \quad (21)$$

In contrast to conventional statistical channel models, where channel impulse responses are built upon a statistical characterization of multipath amplitudes, phases and delays arriving in clusters, etc., the channel impulse response derived from Equation 21 has been obtained directly from the measured channel transfer functions. So, it is expected that this channel impulse response is more accurate than statistical channel modeling, besides that it takes less time and less parameters to construct. From Equation 21, the power delay profile can be obtained as

$$P(\tau) = |h(\tau)|^2 \quad (22a)$$

The mean excess delay is given by

$$\bar{\tau} = \frac{\sum_k P(\tau_k) \tau_k}{\sum_k P(\tau_k)} \quad (22b)$$

and the RMS delay spread is given by

$$\sigma_\tau = \sqrt{\tau^2 - (\bar{\tau})^2} \quad (22c)$$



Fig. 1. Position b with the transmitting antenna in the belly and receiving antenna in the shoulder.

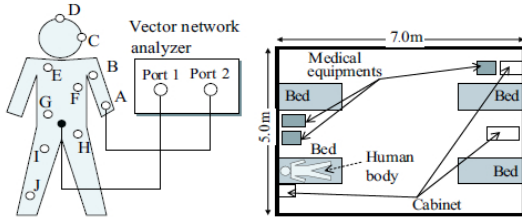


Fig. 2. Hospital room measurements layout.

where

$$\tau^2 = \frac{\sum_k P(\tau_k) \tau_k^2}{\sum_k P(\tau_k)} \quad (22d)$$

The coherent bandwidth for 50% correlation is given by

$$B_c \approx \frac{1}{5 \sigma_\tau} \quad (22e)$$

VII. Simulation Results

As mentioned before, intensive measurement campaigns were performed in NICT. As an example we present the channel transfer functions measured in position b , Figure 1, (for the lower band of UWB) with the transmitting antenna placed in the belly and the receiving antenna placed in the shoulder. Figure 1 illustrates the positions of antennas. The simulations of channel's transfer functions were computed from the measurements performed in a hospital room.

Selecting the order P might be a difficult problem. Monitoring the prediction error variance and model coefficients till they stabilized is difficult to achieve in practice. Nevertheless, from experimental data, the order $P = 5$ was observed to be a best fit.

Thus, a UWB-BAN channel model can be implemented by the AR model described in Equation 18 in the form of a recursive IIR filter implemented as direct form II transposed structure (see Figure 3) with parameters:

- $b_n = \begin{cases} 1 & n = 1 \\ 0 & n \neq 1 \end{cases}$
- $a_1 = -1.3138, a_2 = 0.4829, a_3 = -0.0155, a_4 = -0.1518, a_5 = 0.0650$

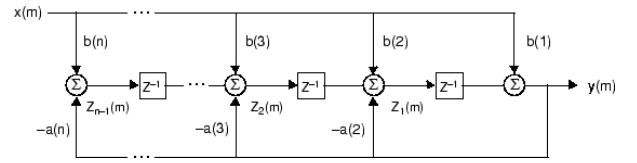


Fig. 3. Direct form II transposed structure.

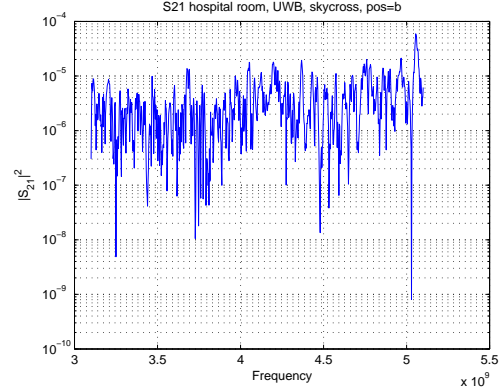


Fig. 4. Measured channel's transfer function in a hospital room and position b .

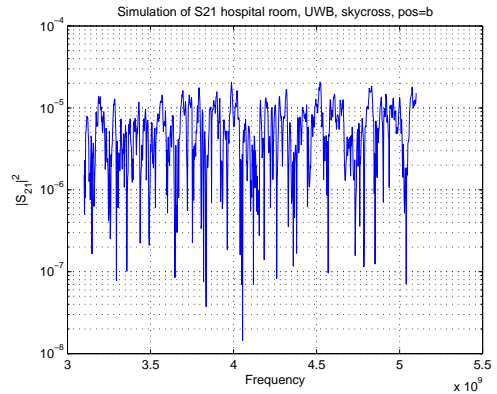


Fig. 5. Simulated channel's transfer function in a hospital room and position b .

- $\sigma_e^2 = 4.853 \times 10^{-12}$
- $x(m) \sim \mathcal{N}(0, \sigma_e^2)$
- $y(m) = H(f_m, d)$

Figures 4 and 5 show the measured and simulated channel's transfer function in a hospital room and position b . Figures 4 and 5 illustrate the measured and simulated channel's impulse response in a hospital room and position b .

VIII. Conclusions

Taking advantage that UWB channels for BANs behave as linear systems, an alternative form of channel modeling is by linear prediction of the channel's transfer function obtained from measurements. An ARMA synthesis method is shown to provide a good fit. Channel impulse responses derived from an ARMA channel model are more accurate than a statistical channel model. Indeed, as this ARMA channel model is derived

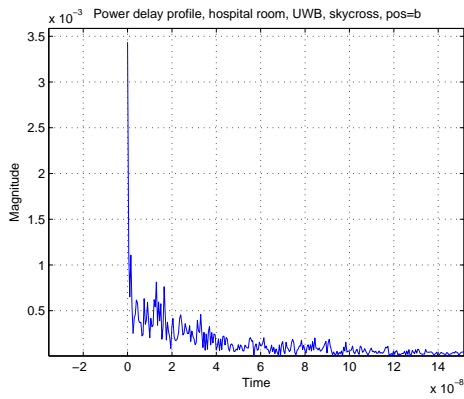


Fig. 6. Measured power delay profile in a hospital room and position b.

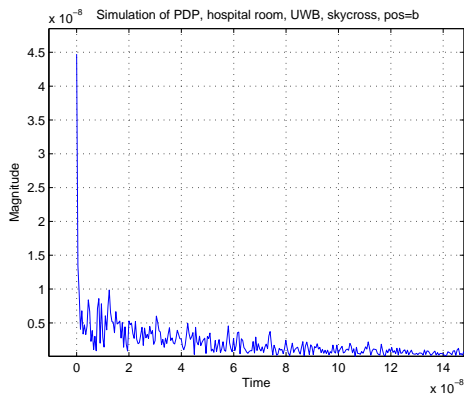


Fig. 7. Simulated power delay profile in a hospital room and position b.

directly from measured channel transfer functions. So, it is expected that this channel impulse response is more accurate. Statistical channel models have some degree of error depending how precise the statistical characterization is done. Moreover, the proposed technique takes less time and less parameters to implement channel impulse responses for simulations. Besides, all propagation's phenomena are embedded into a *simple* model for simulation.

References

- [1] P. Stoica, R. Moses, *Introduction to Spectral Analysis*, Prentice Hall, ISBN 0-13-258419-0.
- [2] P. Bello, "Characterization of randomly time-variant linear channels", *IEEE Transactions on Communications*, Vol 11, No 4, 1963, pp. 360-393.
- [3] S. Howard, K. Pahlavan, "Autoregressive Modeling of Wideband Indoor Radio Propagation", *IEEE Transactions on Communications*, Vol 40, September 1992, pp. 1540-1552.
- [4] W. Turin, et.al., "Autoregressive Modeling of An Indoor UWB Channel", *IEEE Conference on UWB Systems and Technologies*, Baltimore, May 2002, pp. 71-74.
- [5] J. Cavers, *Mobile Channel Characteristics*, Kluwer Academic Publishers, ISBN 0-7923-7926-8.